The unusually favorable interactions of the facial iodides with the tungsten atoms imply that there is metal cluster back-bonding to the ligands, using empty d orbitals on iodide to accept electron density from the electron-rich tungsten(II) unit. The emission energy ordering can be explained in this way, since iodide should be a better π-acceptor than chloride; d–d π-bonding would lower the energy of the HOMO, resulting in a larger energy gap for the tungsten iodide cluster.

Acknowledgment. We thank Miriam Heinrichs, Mike Hopkins, and Dan Nocera for many helpful discussions. T.C.Z. acknowledges a graduate fellowship from the Sun Co. This research was supported by National Science Foundation Grants CHE84-19828 (H.B.G.), CHE82-19039 (X-ray facility), and the Exxon Educational Foundation (W.P.S., B.S.).

Registry No. $[(n\text{-}C_4H_9)_4N]_2W_6Cl_{14}$, 84648-02-2; $[(n\text{-}C_4H_9)_4N]_2W_6Br_{14}$, 96390-92-0; $[(n\text{-}C_4H_9)_4N]_2W_6I_{14}$, 27680-20-2.

Supplementary Material Available: Tables of stucture factors and anisotropic thermal parameters for the refined atoms (61 pages). Ordering information is given on any current masthead page.

Contribution No. 7216 from the Arthur Amos Noyes Laboratory,
California Institute of Technology, Pasadena, California 91125

Preparation and Properties of $[((C_6H_5)_3P)_2N]W_6Br_{14}$

Thomas C. Zietlow, William P. Schaefer, Behzad Sadeghi, Daniel G. Nocera, and Harry B. Gray*

Received June 26, 1985

$(PPN)W_6Br_{14}$ [PPN = $((C_6H_5)_3P)_2N^+$] was prepared by the reaction of $(PPN)_2W_6Br_{14}$ and $NOPF_6$ in degassed methylene chloride solution. $(PPN)W_6Br_{14}$ crystallizes in the monoclinic space group $P2_1/n$ with $a = 9.577$ (2) Å, $b = 22.478$ (6) Å, $c = 24.430$ (4) Å, $\beta = 97.42$ (2)°, and $Z = 4$. The tungsten–tungsten bonds are longer in $W_6Br_{14}^-$ than in $W_6Br_{14}^{2-}$ [d(W–W): $W_6Br_{14}^-$ = 2.649 (8) Å; $W_6Br_{14}^{2-}$ = 2.635 (7) Å], consistent with the electron being removed from a metal–metal bonding orbital. The metal–bromide bonds are shorter in the monoanion than in the dianion [d(W–Br(axial)): $W_6Br_{14}^-$ = 2.538 (12) Å; $W_6Br_{14}^{2-}$ = 2.587 (4) Å], probably due to the greater electrostatic attraction of the halide to the oxidized metal cluster. The electronic absorption spectra of $W_6Br_{14}^-$ and related cluster monoanions indicate that the lowest energy allowed transition [551 nm (ϵ = 2560 M^{-1} cm^{-1}) for $W_6Br_{14}^-$ in CH_2Cl_2] is ligand-to-metal charge transfer from an axial halide. The magnetic properties (EPR, magnetic susceptibility) of $(PPN)W_6Br_{14}$ are consistent with a ^2E ground state.

The nature of the structural distortion in the emissive excited states of the $M_6X_{14}^{2-}$ (M = Mo, W; X = Cl, Br, I) clusters is not known.[1] Because it is likely that this excited state has one electron removed from the $M_6X_{14}^{2-}$ highest occupied molecular orbital,[1c] the one-electron-oxidized clusters ($M_6X_{14}^-$) should reveal at least certain aspects of the distortion in the emissive species. Accordingly, we have performed a crystal structure analysis of one of the oxidized compounds, $(PPN)W_6Br_{14}$ [PPN = $((C_6H_5)_3P)_2N^+$], which is reported here along with the electronic absorption spectra of several oxidized tungsten cluster complexes. Additional information about the electronic structure of $(PPN)W_6Br_{14}$ has been extracted from a 9 K EPR spectrum and variable-temperature magnetic susceptibility measurements.

Experimental Section

Optical absorption spectra were recorded on a Cary 17 spectrometer. Electron paramagnetic resonance spectra were measured on a Varian E-Line Century Series spectrometer equipped with an Air-Products Heli-Tran cooling system. Variable-temperature susceptibility measurements were made at the University of Southern California on a SQUID-based (SHE Corp.) Model 805 variable-temperature susceptometer with a 2 K option.

$(PPN)_2W_6Br_{14}$ was synthesized by mixing W_6Cl_{12} (0.50 g) in an evacuated tube with a 20-fold excess of LiBr:KBr (40:60 mixture) (3.07 g:2.86 g) and heating the sealed tube at 360 °C for 30 min. After cooling, the tube was broken and the contents dissolved in 6 M HBr. This solution was treated with (PPN)Cl, causing a precipitate to form; the solid material was filtered off, dried in vacuo, and recrystallized from methylene chloride/petroleum ether.

$(PPN)W_6Br_{14}$ was synthesized by reacting $(PPN)_2W_6Br_{14}$ with $NOPF_6$ in degassed methylene chloride solution. Crystallization of the product by layering with petroleum ether resulted in deep red crystals. (A few yellow crystals of starting material also were obtained; these were carefully dissolved off with acetonitrile.) Anal. Calcd for $C_{36}H_{30}P_2NW_6Br_{14}$: C, 15.55; H, 1.10; N, 0.51. Found: C, 16.14; H, 1.17; N, 0.51.

$(TBA)W_6Cl_{14}$, $(TBA)W_6Cl_8Br_6$, and $(TBA)W_6Br_8Cl_6$ [TBA = $(C_4H_9)_4N^+$] were generated by $NOPF_6$ oxidation of the corresponding cluster dianions in degassed methylene chloride solution.[2]

Table I. Crystal Data for $[Ph_3P{=}N{=}PPh_3][W_6Br_{14}]$

formula: $W_6Br_{14}P_2NC_{36}H_{30}$
$a = 9.577$ (5) Å
$b = 22.478$ (12) Å
$c = 24.430$ (8) Å
$\beta = 97.42$ (2)°
$V = 5215$ (6) Å^3
$\mu = 253.5$ cm^{-1}

$F(000) = 4868$ e
fw = 2760.43
space group: $P2_1/n$ (No. 14)
$T = 21$ °C
λ(Mo Kα) = 0.71073 Å
$d_{\mathrm{exptl}} = 3.47$ g cm^{-3}

X-ray Structure Determination. A crystal 0.23 × 0.28 × 0.20 mm with faces {011} and (10$\bar{1}$), ($\bar{1}$01) was chosen. Preliminary photographs showed a monoclinic cell; the crystal was transferred to a Nicolet P2$_1$ diffractometer equipped with graphite-monochromated Mo Kα radiation, and unit cell dimensions were obtained from the setting angles of 15 reflections with $20° < 2\theta < 30°$. Crystal data are given in Table I. Systematic absences in the diffractometer data of $h0l$, $h + l = 2n + 1$, and $0k0$, $k = 2n + 1$, indicate space group $P2_1/n$, a special setting of No. 14, with equivalent positions $\pm(x, y, z; {}^1/_2 - x, {}^1/_2 + y, {}^1/_2 - z)$. A total of 11 670 reflections with $2\theta < 40°$ in quadrants $h,k,\pm l$ and $h,-k,\pm l$ were measured with ω scans 1° wide at 1°/min. Three check reflections were monitored every 97 reflections and showed no variations greater than those expected statistically. The data were corrected for absorption by Gaussian integration over an 8 × 8 × 8 grid (transmission factors ranged from 0.013 to 0.044) and Lorentz and polarization factors were applied. The data were merged to give 4875 independent reflections, all of which were used in the structure solution and refinement; the goodness of fit

---

[1] (a) Maverick, A. W.; Gray, H. B. *J. Am. Chem. Soc.* **1981**, *103*, 1298. (b) Maverick, A. W.; Najdzionek, J. S.; MacKenzie, D.; Nocera, D. G.; Gray, H. B. *J. Am. Chem. Soc.* **1983**, *105*, 1878. (c) Zietlow, T. C.; Hopkins, M. D.; Gray, H. B. *J. Solid State Chem.* **1985**, *57*, 112.

[2] The initial products of oxidation of the other $(TBA)_2W_6X_8Y_6$ clusters decomposed at room temperature in dichloromethane solution as evidenced by changing electronic absorption spectral features with time. The reported data are for spectra that did not change over several days in solution.

0020-1669/86/1325-2198$01.50/0

Table II. Final Parameters for $[((C_6H_5)_3P)_2N]W_6Br_{14}$[a]

atom	x	y	z	U_{eq} or B, Å^2
W(1)	58844 (7)	6331 (3)	46786 (3)	259 (2)
W(2)	50234 (8)	4413 (3)	56486 (3)	272 (2)
W(3)	32295 (7)	3205 (3)	47418 (3)	272 (2)
W(4)	43765 (8)	48054 (3)	56729 (3)	316 (2)
W(5)	48770 (8)	41957 (3)	47922 (3)	313 (2)
W(6)	68657 (8)	48897 (3)	53152 (3)	307 (2)
Br(1)	40952 (20)	5099 (9)	37853 (7)	424 (5)
Br(2)	76553 (20)	7353 (9)	55853 (7)	432 (5)
Br(3)	50069 (25)	10650 (10)	65156 (8)	622 (6)
Br(4)	41550 (21)	13726 (9)	50534 (8)	463 (5)
Br(5)	70707 (23)	15049 (9)	42608 (8)	545 (6)
Br(6)	75743 (19)	−1265 (9)	42917 (7)	441 (5)
Br(7)	8246 (22)	7549 (11)	44280 (10)	645 (7)
Br(8)	24230 (21)	41291 (9)	51501 (8)	490 (5)
Br(9)	61038 (21)	39092 (9)	57748 (8)	497 (5)
Br(10)	73412 (21)	42885 (9)	44477 (8)	508 (5)
Br(11)	35427 (27)	45334 (12)	65816 (8)	760 (7)
Br(12)	36652 (24)	45105 (10)	38177 (8)	575 (6)
Br(13)	46553 (26)	31029 (10)	45028 (9)	652 (7)
Br(14)	93904 (22)	47631 (11)	57522 (9)	691 (6)
P(1)	6080 (5)	3035 (2)	2395 (2)	2.6 (1)
P(2)	4156 (5)	2014 (2)	2323 (2)	2.5 (1)
N	5103 (15)	2540 (6)	2596 (5)	3.0 (3)
C(11)	6806 (20)	2867 (9)	1753 (7)	4.0 (4)
C(12)	7884 (22)	2432 (9)	1802 (8)	4.9 (5)
C(13)	8342 (25)	2250 (11)	1284 (9)	6.1 (6)
C(14)	7793 (26)	2488 (11)	797 (9)	6.3 (6)
C(15)	6672 (22)	2901 (9)	764 (8)	4.8 (5)
C(16)	6136 (20)	3090 (9)	1249 (7)	4.0 (4)
C(21)	7505 (18)	3138 (7)	2931 (6)	2.6 (4)
C(22)	7447 (19)	2909 (8)	3443 (7)	3.3 (4)
C(23)	8544 (22)	3004 (9)	3862 (8)	4.4 (5)
C(24)	9746 (23)	3345 (10)	3761 (8)	5.0 (5)
C(25)	9816 (24)	3564 (11)	3247 (9)	6.0 (6)
C(26)	8717 (20)	3465 (9)	2801 (7)	4.1 (4)
C(31)	5126 (19)	3727 (8)	2290 (7)	3.5 (4)
C(32)	3824 (20)	3774 (8)	2487 (7)	3.7 (4)
C(33)	3080 (21)	4337 (9)	2410 (8)	4.7 (5)
C(34)	3691 (21)	4786 (9)	2186 (8)	4.6 (5)
C(35)	4957 (24)	4745 (11)	1944 (8)	5.8 (5)
C(36)	5725 (22)	4196 (10)	2019 (8)	5.0 (5)
C(41)	5066 (16)	1315 (7)	2426 (6)	2.0 (3)
C(42)	6282 (18)	1290 (8)	2788 (7)	2.9 (4)
C(43)	6915 (12)	737 (9)	2912 (7)	3.8 (4)
C(44)	6352 (21)	226 (9)	2649 (8)	4.4 (4)
C(45)	5131 (22)	242 (9)	2257 (8)	4.7 (5)
C(46)	4465 (10)	809 (9)	2154 (7)	3.8 (4)
C(51)	2641 (19)	1941 (8)	2678 (6)	3.1 (4)
C(52)	2730 (20)	2177 (8)	3218 (7)	3.7 (4)
C(53)	1593 (22)	2059 (9)	3528 (8)	4.7 (5)
C(54)	430 (22)	1738 (9)	3278 (8)	4.4 (5)
C(55)	378 (22)	1531 (9)	2758 (8)	4.7 (5)
C(56)	1486 (20)	1647 (9)	2451 (7)	3.9 (4)
C(61)	3577 (18)	2111 (8)	1591 (6)	2.6 (4)
C(62)	2515 (20)	2519 (9)	1445 (7)	3.9 (4)
C(63)	2151 (21)	2664 (9)	871 (8)	4.4 (5)
C(64)	2835 (22)	2399 (9)	498 (8)	4.6 (5)
C(65)	3884 (21)	1991 (9)	630 (7)	4.1 (4)
C(66)	4316 (18)	1836 (8)	1212 (7)	3.1 (4)

[a] Tungsten and bromine positional parameters have been multiplied by 10^5; other positional parameters and all U_{eq} by 10^4. $U_{eq} = {}^1/_3 \cdot [\sum_i \sum_j U_{ij}(a_i{}^* a_j{}^*)(\vec{a}_i \vec{a}_j)]$ and $\sigma(U_{eq}) = (1/6^{1/2})\langle \sigma(U_{ii})/U_{ii} \rangle U_{eq}$.

for merging was 1.34. Variances were assigned to the values of $F_o{}^2$ based on counting statistics plus an additional term $(0.02I)^2$, to account for errors proportional to intensity.

The structure was solved by MULTAN[3] after the Patterson map proved difficult to interpret. With $z = 4$ in the space group $P2_1/n$, no special symmetry was imposed on the molecule. The PPN$^+$ cations are in general positions, but there are two independent anions that are located at two different centers of symmetry; hence the anions are centrosymmetric. The MULTAN solution gave all six tungsten atoms; subsequent structure factor–Fourier calculations located the 14 bromine atoms and the 39 non-hydrogen atoms of the cation. Several cycles of least-squares refinement minimizing $\sum w(k^2F_o{}^2 - F_c{}^2)^2$, where k is a scale factor, with tungsten and bromine atoms given anisotropic thermal parameters, led to convergence with an R ($= \sum|F_o - |F_c||/\sum F_o$) value of 0.046 for all reflections with $F_o{}^2 > 0$ and 0.031 for the 4580 data with $F_o{}^2 > 3\sigma(F_o{}^2)$. The weighted R index, $\sum w(F_o{}^2 - F_c{}^2)/\sum wF_o{}^2$ ($F_o{}^2 > 0$) is 0.0042. The goodness of fit ($=[\sum w(F_o{}^2 - F_c{}^2)^2/(n - p)]^{1/2}$) is 1.40 for $n = 4869$ reflections and $p = 337$ parameters (six strong, low-angle reflections were given zero weight in the refinement). Final parameters are given in Table II; bond lengths in the anion are listed in Table III. Scattering factors for neutral W, Br, P, N, and C were taken from ref 4, the values for W

Table III. Bond Lengths (Å) in the Anion

anion I			anion II		
atom	atom	dist	atom	atom	dist
W(1)	W(2)	2.643 (1)	W(4)	W(5)	2.646 (1)
	W(3)	2.662 (1)		W(6)	2.650 (1)
	W(2′)	2.655 (1)		W(5′)	2.656 (1)
	W(3′)	2.648 (1)		W(6′)	2.640 (1)
W(2)	W(3)	2.636 (1)	W(5)	W(6)	2.658 (1)
	W(3′)	2.656 (1)		W(6′)	2.640 (1)
W(1)	Br(5)	2.544 (2)	W(4)	Br(11)	2.529 (3)
W(2)	Br(3)	2.542 (2)	W(5)	Br(13)	2.557 (2)
W(3)	Br(7)	2.528 (2)	W(6)	Br(14)	2.530 (2)
Br(1)	W(1)	2.610 (2)	Br(8)	W(4)	2.613 (2)
	W(2′)	2.626 (2)		W(5)	2.616 (2)
	W(3)	2.613 (2)		W(6)	2.621 (2)
Br(6)	W(1)	2.612 (2)	Br(9)	W(4)	2.598 (2)
	W(2′)	2.609 (2)		W(5)	2.613 (2)
	W(3′)	2.613 (2)		W(6)	2.620 (2)
Br(2)	W(1)	2.620 (2)	Br(10)	W(4′)	2.611 (2)
	W(2)	2.630 (2)		W(5)	2.614 (2)
	W(3′)	2.600 (2)		W(6)	2.603 (2)
Br(4)	W(1)	2.596 (2)	Br(12)	W(4′)	2.613 (2)
	W(2)	2.622 (2)		W(5)	2.608 (2)
	W(3)	2.605 (2)		W(6′)	2.616 (2)
W(1)	W(1′)	3.758 (1)	W(4)	W(4′)	3.744 (1)
W(2)	W(2′)	3.734 (1)	W(5)	W(5′)	3.755 (1)
W(3)	W(3′)	3.750 (1)	W(6)	W(6′)	3.737 (1)

	I	II	av dist
W–W(cis)	2.650 (9)	2.648 (8)	2.649 (8)
W–W(trans)	3.747 (12)	3.745 (9)	3.746 (10)
W–Br(axial)	2.538 (9)	2.539 (16)	2.538 (12)
W–Br(facial)	2.614 (9)	2.611 (6)	2.613 (8)

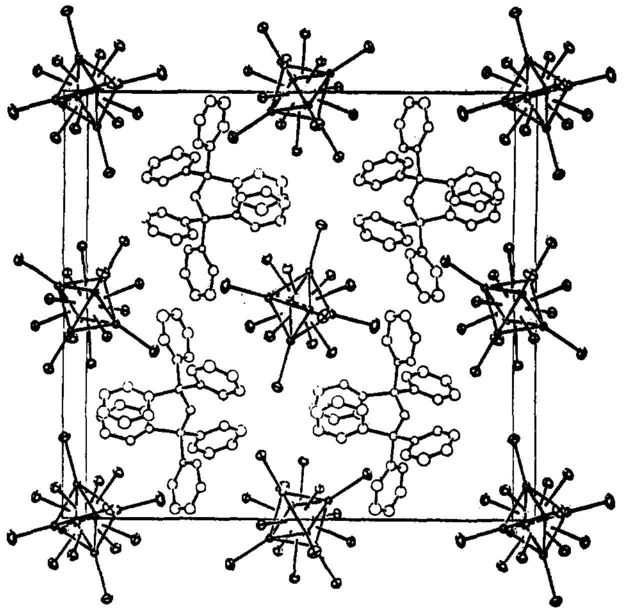

Figure 1. ORTEP view of the unit cell of $(PPN)W_6Br_{14}$ approximately down a, with the unit cell outlined (30% probability thermal ellipsoids are shown).

---

(3) Main, P.; Woolfson, M. M.; Lessinger, L.; Germain, G.; Declercq, J.-P.; Hull, S. E. *MULTAN 78*; University of York: York, England.

(4) *International Tables for Crystallography*; Kynoch: Birmingham, England, 1974; Vol. IV, p 72.

Table IV. Electronic Absorption Spectral Data[a]

complex	λ_{max}, nm	$\bar{\nu}_{max}$, cm^{-1}	ϵ, M^{-1} cm^{-1}
$(TBA)W_6Cl_{14}$	400	25 000	3010
	352	28 400	3870
$(TBA)W_6Cl_8Br_6$	518	19 300	3200
	450	22 200	2880
$(TBA)W_6Br_8Cl_6$	454	22 000	2340
	368	27 200	4490
$(PPN)W_6Br_{14}$	551	18 200	2560
	460	21 700	2220
	441	22 700	2200
	295	33 900	9020

[a] All spectra recorded in methylene chloride solution at 22 °C.

being decreased by 1.421 electrons, for Br being decreased by 0.374 electron, and for P being increased by 0.090 electron to correct for the real part of anomalous dispersion.

Analytical Procedures. Carbon, hydrogen, and nitrogen analyses were performed at the Analytical Laboratory, California Institute of Technology.

Results and Discussion

An ORTEP drawing of the contents of the unit cell of $(PPN)W_6Br_{14}$ is shown in Figure 1. The two independent anions are equivalent within experimental error, and the following discussion will use average bond distances for the two. The tungsten atoms for a nearly regular octahedron with W–W (cis) distances of 2.649 (8) Å, with maximum deviations of 0.013 Å from this average. The trans W–W distances average 3.746 (10) Å, with a maximum deviation from this of 0.012 Å. The longest trans W–W distances are associated with the longest W–Br(axial) distances, but no other correlations are evident. The deviations we see, however, are greater than the esd's in individual W–W distances given in Table III (0.001 Å). It is possible that there is a small molecular distortion that is not large enough to cause the distorted ions to be ordered in the crystal, and the X-ray structure then is some average over several orientations of the real structure. Such a disorder would be expected to show itself in abnormal thermal parameters of the tungsten or bromine atoms. These parameters, however, are not abnormal; thus we conclude that the small departures from regularity in this ion are random.

The $PPh_3{=}N{=}PPh_3^+$ cation in this structure shows normal bond distances and angles with moderately large standard deviations. The two N=P bonds average 1.578 (14) Å, and the six P–C bonds average 1.804 (19) Å; both distances are normal. The C–C distances in the phenyl rings average 1.39 (4) Å, and the rings are all planar within 0.05 Å. The isotropic thermal parameters of the phosphorus nitrogen and inner carbon atoms average about 3 Å^2 while the carbon atoms farthest from the phosphorus atoms have values of about 5 Å^2. The closest Br–C approach is 3.4 Å, and the closest nonbonded C–C approach is 3.2 Å; the Br–C distance is at the short end of a van der Waals contact while the C–C distance is normal.

The most prominent feature of the electronic absorption spectrum of $(PPN)W_6Br_{14}$ in dichloromethane is a broad band with λ_{max} = 551 nm. This absorption, which is responsible for the deep burgundy color of the solution, is probably due to a ligand-to-metal charge-transfer transition from a Br-based MO to the partially occupied e_g orbital[1c] on the metal core. Solution spectroscopic data for several cluster monoanions are given in Table IV.

When the terminal halide is changed from chloride to bromide, the band red shifts by 5700 (W_6Cl_8 core) and 3800 cm^{-1} (W_6Br_8 core), with very little change in the extinction coefficient. Changing the bridging halides while keeping the same terminal ligand results in a much smaller shift in $\bar{\nu}_{max}$ for the lowest energy absorption, 2970 ($W_6Cl_{14}^-$ to $W_6Br_8Cl_3^-$) and 1150 cm^{-1} ($W_6Cl_8Br_6^-$ to $W_6Br_{14}^-$), with the extinction coefficients of the W_6Br_8 core about 25% lower than the corresponding values for W_6Cl_8. These data indicate that the charge transfer is mainly from a terminal ligand, since the energy of the transition decreases significantly upon replacement of the terminal chlorides by bromides. The lower extinction coefficients of the absorptions in $W_6Br_8X_6^-$ with respect to $W_6Cl_8X_6^-$ may result from decreased overlap of the tungsten and terminal halide orbitals due to the steric bulk of the larger halides.

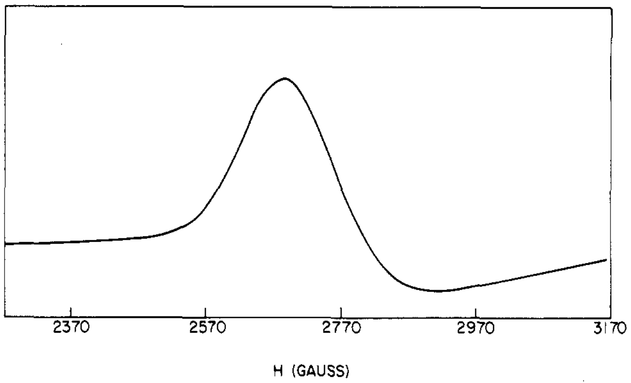

Figure 2. EPR spectrum of $(PPN)W_6Br_{14}$ in frozen methylene chloride solution at 9 K (9.182 GHz).

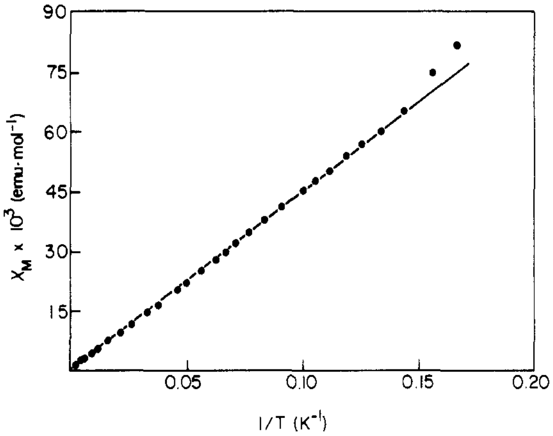

Figure 3. Variable-temperature magnetic susceptibility data for powdered $(PPN)W_6Br_{14}$.

Table V. Bond Distances (Å) in $W_6Br_{14}^{2-}$ and $W_6Br_{14}^-$

bond	$W_6Br_{14}^{2-}$	$W_6Br_{14}^-$
W–W(cis)	2.635 (7)	2.649 (8)
W–W(trans)	3.726 (4)	3.746 (10)
W–Br(axial)	2.587 (4)	2.538 (12)
W–Br(facial)	2.628 (9)	2.613 (8)

The EPR spectrum of $(PPN)W_6Br_{14}$ in frozen methylene chloride solution at 9 K is shown in Figure 2. Raising the temperature of the sample causes the EPR spectrum to broaden and finally to be indistinguishable from the base line at 25 K. The EPR spectrum at 9 K is only slightly anisotropic. Variable-temperature magnetic susceptibility data are plotted in Figure 3. There appears to be a transition point in the data at very low temperatures where μ_{eff} becomes significantly greater than the spin-only value (1.73 μ_B). Such behavior is consistent with a ^2E ground state.[6]

Anisotropic EPR data indicate[1] that the structure of $Mo_6Cl_{14}^-$ is axially compressed relative to that of $Mo_6Cl_{14}^{2-}$. However, the crystal structure of $(PPN)W_6Br_{14}$, as well as the magnetic data, does not reveal a specific axial compression. The lack of unusually large thermal ellipsoids suggests that the distortion, if there is one, is not large enough to be "frozen" at low temperatures.

The $W_6Br_{14}^{2-}$ and $W_6Br_{14}^-$ bond lengths (Table V)[5] provide information about the electronic structures[7] of these types of

---

(5) Zietlow, T. C.; Schaefer, W. P.; Sadeghi, B.; Hua, N.; Gray, H. B. *Inorg. Chem.*, preceding paper in this issue.

(6) Mabbs, F. E.; Machin, D. J. *Magnetism and Transition Metal Complexes*; Chapman and Hall: London, 1973; p 95.

clusters. The monoanion has a slightly enlarged octahedron compared to the dianion, an indication that the electron removed in the oxidation is from a bonding orbital (although the increased charge on the tungsten core would be expected to expand it also). The W–Br(axial) bond is significantly shorter in the monoanion, presumably due to the electrostatic attraction of the negatively charged halide to the now more positively charged W_6 unit. The W–Br(facial) bonds are not significantly shorter in the monoanion despite the higher charge on the metals, possibly because the metal–bromide back-bonding inferred from the $W_6X_{14}^{2-}$ structures[5] and photophysics[8] is diminished in the oxidized metal core. The expected shortening of the metal–bromide(facial) bond upon metal–core oxidation may be compensated by the decrease in the interaction of filled metal orbitals with the empty Br 4d orbitals.

Acknowledgment. T.C.Z. and D.G.N. acknowledge graduate fellowships from the Sun Co. This work was supported by National Science Foundation Grants CHE84-19828 (H.B.G.), CHE82-11349 (USC SQUID Instrumentation Facility), and CHE82-19039 (Caltech X-ray Facility) and the Exxon Educational Foundation (W.P.S., B.S.).

Registry No. $(PPN)_2W_6Br_{14}$, 101955-15-1; W_6Cl_{12}, 12052-19-6; $(PPN)W_6Br_{14}$, 101955-18-4; $(TBA)W_6Cl_{14}$, 101955-24-2; $(TBA)W_6Cl_8Br_6$, 101955-26-4; $(TBA)W_6Br_8Cl_6$, 101955-22-0; $(TBA)_2W_6Cl_{14}$, 84648-02-2; $(TBA)_2W_6Cl_8Br_6$, 101955-16-2; $(TBA)_2W_6Br_8Cl_6$, 101955-20-8.

Supplementary Material Available: A table of anisotropic thermal parameters for refined atoms and electronic spectra of $W_6X_8Y_6^{2-}$ (5 pages). Ordering information is given on any current masthead page.

---

(7) (a) Seifert, G.; Finster, J.; Müller, H. *Chem. Phys. Lett.* **1980**, *75*, 373. (b) Cotton, F. A.; Stanley, G. G. *Ibid.* **1978**, 58, 450. (c) Korol'kov, D.; Pak, V. N. *Zh. Strukt. Khim.* **1973**, *14*, 1098.

(8) Zietlow, T. C.; Nocera, D. G.; Gray, H. B. *Inorg. Chem.*, in press.

Contribution from the Department of Chemistry and Biochemistry,
University of Windsor, Windsor, Ontario N9B 3P4, Canada

Synthesis and Spectroscopic Characterization of Dithiocarbamate Derivatives of Methyl-, Dimethyl-, and Trimethylgermane and Crystal Structure of Dimethylbis(*N*,*N*-dimethyldithiocarbamato)germanium

Raj K. Chadha, John E. Drake,* and Anil B. Sarkar

Received July 18, 1985

Seven organogermanium derivatives of dithiocarbamic acid of the general formula $(CH_3)_nGeX_{4-n-m}[S_2CN(CH_3)_2]_m$ (where X = Cl, Br, I; n = 1–3, m = 1, 2) have been prepared either by the reaction of sodium *N*,*N*-dimethyldithiocarbamate with the appropriate halomethylgermane or in the case of partially substituted bromo and iodo derivatives by halide exchange reactions with bromotrimethylsilane and iodotrimethylsilane. The dithiocarbamates were characterized by vibrational and NMR spectroscopy and mass spectrometry. The ^1H and ^{13}C NMR spectra are consistent with the sulfur atoms undergoing rapid exchange in solution. The vibrational spectra of the halide-containing species suggest the presence of a relatively weak Ge–X bond consistent with the halide occupying the axial position in a distorted pseudo trigonal bipyramid. The crystal structure of $(CH_3)_2Ge[S_2CN(CH_3)_2]_2$ was determined and indicates that the germanium atom is at the center of a distorted octahedron, in contrast to the case of $(CH_3)_2GeCl[S_2CN(CH_3)_2]$, in which the geometry around the germanium atom is that of a distorted pseudo trigonal bipyramid. The compound crystallizes in the orthorhombic space group *Fdd*2 with unit cell parameters (21 ± 1 °C) a = 25.05 (3) Å, b = 34.74 (3) Å, c = 6.896 (6) Å, and V = 6000 (10) Å^3; Z = 16, ρ(obsd) = 1.53 g cm^{-3}, ρ(calcd) = 1.52 g cm^{-3}, and R = 0.0283 for 1107 observed reflections.

Introduction

The structural chemistry of organogermanium derivatives was reviewed in 1983,[1] and only five compounds were mentioned that contain a Ge–S bond. There have been many reports of dithiocarbamates of both transition metals[2–4] and main-group elements,[5] but we recently reported a preliminary note containing the first structure of an organogermanium dithiocarbamate.[6] In $(CH_3)_2GeCl[S_2CN(CH_3)_2]$ the dithiocarbamate group acts in an anisobidentate fashion[6] similar to that found for the tin analogue.[7] In view of the variety of structures found for other tin derivatives,[8] it was of interest to make a more extensive comparative study of the spectroscopic properties of other methylgermanium derivatives and to carry out structural determinations whenever appropriate crystals could be grown. Unfortunately, in only one case were we able to get crystals of the appropriate quality that did not decay rapidly during data collection.

Experimental Section

Starting Materials. Trichloromethylgermane (Alfa) was purified by trapping it out at −23 °C. The other halomethylgermanes (Alfa) were used as supplied as were bromo- and iodotrimethylsilane (Petrarch) and the sodium salt of dimethyldithiocarbamic acid (Kodak). Carbon di-

---

(1) Molloy, K. C.; Zuckermann, J. J. *Adv. Inorg. Chem. Radiochem.* **1981**, *17*, 113.

(2) Willemse, J.; Cras, J. A.; Steggerda, J. J.; Keijzers, C. P. *Struct. Bonding (Berlin)* **1976**, *28*, 83.

(3) Abrahamson, H. B.; Freeman, M. L.; Hossain, M. B.; van der Helm, D. *Inorg. Chem.* **1984**, *23*, 2286 and references therein.

(4) Templeton, J. L.; Herrik, R. S.; Rusik, C. A.; McKenna, C. E.; McDonald, J. W.; Newton, W. E. *Inorg. Chem.* **1985**, *24*, 1383.

(5) Coucouvanis, D. *Prog. Inorg. Chem.* **1970**, *11*, 233.

(6) Chadha, R. K.; Drake, J. E.; Sarkar, A. B. *Inorg. Chem.* **1984**, *23*, 4769.

(7) Furue, K.; Kimura, T.; Yasuoka, N.; Kasai, N.; Kakudo, M. *Bull. Chem. Soc. Jpn.* **1970**, *43*, 1661.

(8) (a) Sheldrick, G. M.; Sheldrick, W. S. *J. Chem. Soc. A* **1970**, 490. (b) Sheldrick, G. M.; Sheldrick, W. S.; Dalton, R. F.; Jones, K. *J. Chem. Soc. A* **1970**, 493. (c) Morris, J. S.; Schlemper, E. O. *J. Cryst. Mol. Struct.* **1979**, *9*, 1, 13. (d) Harreld, C. S.; Schlemper, E. O. *Acta Crystallogr., Sect. B: Struct. Crystallogr. Cryst. Chem.* **1971**, *B27*, 1964.